Dissociable Contribution of Extrastriate Responses to Representational Enhancement of Gaze Targets

Yaser Merrikhi[1*], Mohammad Shams-Ahmar[2,3*], Hamid Karimi-Rouzbahani[3,4,5*], Kelsey Clark[6], Reza Ebrahimpour[2,7], and Behrad Noudoost[6]

Abstract

■ Before saccadic eye movements, our perception of the saccade targets is enhanced. Changes in the visual representation of saccade targets, which presumably underlie this perceptual benefit, emerge even before the eye begins to move. This perisaccadic enhancement has been shown to involve changes in the response magnitude, selectivity, and reliability of visual neurons. In this study, we quantified multiple aspects of perisaccadic changes in the neural response, including gain, feature tuning, contrast response function, reliability, and correlated activity between neurons. We then assessed the contributions of these various perisaccadic modulations to the population's enhanced perisaccadic representation of saccade targets. We found a partial dissociation between the motor information, carried entirely by gain changes, and visual information, which depended on all three types of modulation. These findings expand our understanding of the perisaccadic enhancement of visual representations and further support the existence of multiple sources of motor modulation and visual enhancement within extrastriate visual cortex. ■

INTRODUCTION

The deployment of visuospatial attention is tightly linked with the execution of saccadic eye movements (Awh, Armstrong, & Moore, 2006). Numerous studies have shown that shifts in attention precede eye movements, improving both the sensitivity to and discriminability of visual targets of the upcoming saccade (Stewart, Verghese, & Ma-Wyatt, 2019; Born, Ansorge, & Kerzel, 2013; Peterson, Kramer, & Irwin, 2004; Deubel & Schneider, 1996; Hoffman & Subramaniam, 1995) and promoting their entry into working memory (Hanning, Jonikaitis, Deubel, & Szinte, 2016). To what extent the neural basis of this presaccadic boost in perception, that is, overt attention, overlaps with that of covert attention has not been examined. The gain and reliability of visual responses increase during both covert and overt attention (Steinmetz & Moore, 2010). Moreover, receptive fields (RFs) shift toward those targets (Neupane, Guitton, & Pack, 2016a, 2016b; Zirnsak, Steinmetz, Noudoost, Xu, & Moore, 2014; Steinmetz & Moore, 2010; Moore & Chang, 2009; Sheinberg & Logothetis, 2001; Tolias et al., 2001; Moore, 1999; Moore, Tolias, & Schiller, 1998; Chelazzi, Miller, Duncan, & Desimone, 1993; Fischer & Boch, 1981). This strong resemblance between perisaccadic changes in visual responses and those observed during covert attention emphasizes the degree of overlap between neural substrates utilized by both attentional mechanisms. Importantly, covert attention has been argued to improve behavioral performance primarily by reducing interneuronal correlations. Recording the activity of extrastriate neurons in monkeys performing a covert attention task, Cohen and Maunsell assessed the contribution of changes at the level of single neuronal responses, as well as the population, to enhancing sensory signals (Cohen & Maunsell, 2009). They specifically evaluated the contribution of response gain (measured by the firing rate [FR]), response reliability (assessed using the Fano factor [FF]), and correlated activity (measured as noise correlation) and found that the decrease in correlated activity is the largest contributor to the attentional enhancement.

Overt orientation of gaze toward the targets of attention is an extremely common form of attention, occurring approximately 3 times per second. Therefore, we sought to determine the degree to which various changes in the response of visual neurons contribute to the perisaccadic enhancement of saccade targets, that is, the overt attention targets. We also sought to establish the generalizability of this perisaccadic enhancement by recording from a dorsal stream area, the middle temporal (MT) area, which occupies

[1]Department of Physiology, McGill University, Montréal, Canada, [2]School of Cognitive Sciences, Institute for Research in Fundamental Sciences (IPM), Tehran, Iran, [3]Department of Cognitive Neurology, Hertie Institute for Clinical Brain Research, University of Tübingen, Germany, [4]Perception in Action Research Centre, Department of Cognitive Science, Macquarie University, Australia, [5]Medical Research Council Cognition and Brain Sciences Unit, University of Cambridge, UK, [6]Department of Ophthalmology and Visual Sciences, University of Utah, Salt Lake City, Utah, [7]Faculty of Computer Engineering, Shahid Rajaee Teacher Training University, Tehran, Iran
*These authors contributed equally to the paper.

Journal of Cognitive Neuroscience 33:10, pp. 2167–2180
https://doi.org/10.1162/jocn_a_01750

a position in the visual hierarchy similar to V4, where perisaccadic enhancement has previously been reported. We recorded responses from visual area MT during a visually guided saccade task with visual probes, similar to previous studies (Steinmetz & Moore, 2010; Moore & Chang, 2009; Moore et al., 1998). We assessed the feature tuning, contrast response functions, and correlated variability of visual responses just before eye movements either toward or away from neurons' RFs. To better compare our findings with prior covert attention studies, we employed a computational method similar to that developed by Cohen and Maunsell (Cohen & Maunsell, 2009) to quantify the contribution of each perisaccadic modulation to the enhanced visual representation. This approach revealed a differential contribution of response gain, reliability, and correlated activity to motor and visual information during overt attention.

METHODS

General and Surgical Procedures

Two adult male rhesus monkeys (*Macaca mulatta*) were used in this study. All experimental procedures were in accordance with the National Institutes of Health Guide for the Care and Use of Laboratory Animals, and the Society for Neuroscience Guidelines and Policies. The protocols for all experimental, surgical, and behavioral procedures were approved by the Montana State University Institutional Animal Care and Use Committee. All surgical procedures were carried out under isoflourane anesthesia and strict aseptic conditions. Before undergoing behavioral training, each animal was implanted with a stainless steel headpost (Gray Matter Research), attached to the skull using orthopedic titanium screws and dental acrylic. Following behavioral training, custom-made recording chambers (interior 22 × 22 mm) were mounted on the skull and affixed with dental acrylic. Within the chambers, two 22 × 22 mm craniotomies were performed above the extrastriate visual areas (extrastriate craniotomies were centered at −6-mm A/P, 23-mm M/L and −13-mm A/P, 23-mm M/L).

Behavioral Monitoring

Animals were seated in a custom-made primate chair, with their head restrained and a tube to deliver juice rewards placed in their mouth. Eye position was monitored with an infrared optical eye tracking system (EyeLink 1000 Plus Eye Tracker, SR Research Ltd) and stored at 2 kHz. The EyeLink PM-910 Illuminator Module and EyeLink 1000 Plus Camera (SR Research Ltd) were mounted above the monkey's head and captured eye movements via an angled infrared mirror. Juice was delivered via a syringe pump and the Syringe PumpPro software (NE-450 1L-X2, New Era Pump Systems, Inc.). Stimulus presentation and juice delivery were controlled using custom software, written in MATLAB (The MathWorks) using the MonkeyLogic toolbox (Asaad, Santhanam, McClellan, & Freedman, 2013). Visual stimuli were presented on an LED-lit monitor (Asus VG248QE: 24 in., resolution 1920 × 1080, 144-Hz refresh rate), positioned 28.5 cm in front of the animal's eyes. A photodiode (OSRAM Opto Semiconductors) was used to record the actual time of stimulus appearance on the monitor, with a continuous signal sampled and stored at 32 kHz.

Neurophysiological Recording Setup

The electrode was mounted on the recording chamber and positioned within the craniotomy area using a Narishige two-axis platform allowing continuous adjustment of the electrode position. For single electrode recordings, a 28-gauge guide tube was lowered to contact or just penetrate the dura, using a manual oil hydraulic micromanipulator (Narishige). Then, a varnish-coated tungsten microelectrode (FHC), shank diameter 200–250 μm, impedance 0.2–1 MΩ (measured at 1 kHz), was advanced into the brain for the extracellular recording of neuronal activity. Single-electrode recordings used a Plexon pre-amplifier and AM Systems amplifier, filtering from 300 to 5 kHz. For array electrode recordings, a 28-gauge guide tube was lowered as described, and the 16-channel linear array electrode (V-probe, Plexon, Inc.) was advanced into the brain using the hydraulic microdrive; array contacts were spaced 150 μm apart. The array electrode was connected to a headstage pre-amplifier (Neuralynx, Inc.). Neuralynx Digital Lynx SX and associated software were used for data acquisition. Spike waveforms and continuous data were digitized and stored at 32 kHz for off-line spike sorting and data analysis. Spike waveforms were sorted manually using an off-line sorter (Plexon). Area MT was identified based on stereotaxic location, position relative to nearby sulci, patterns of gray and white matter, and motion selectivity of units encountered.

We recorded from 84 MT single units across 13 recording sessions, for 271 pairs of simultaneously recorded neurons (mean ~7 neurons per session; 48 neurons and eight sessions in Monkey 1, 36 neurons and five sessions in Monkey 2). Only neurons with visual responses to the stimuli were included in the analysis; units were audibly screened for visual responses during electrode positioning, and stimulus position was placed based on a preliminary estimate of the RF of neurons being recorded (see below).

Behavioral Tasks

Eye Calibration

The fixation point, a ~1-dva radius white circle, appeared in the center of the screen, and the monkey maintained fixation within a 1.5-dva radius circular window for 1.5 sec. For eye calibration, the fixation point could appear either

centrally or offset by 10 dva in the vertical or horizontal axis. The monkey was rewarded for maintaining fixation.

Preliminary RF Mapping

Preliminary RF mapping was conducted by having the monkey fixate within a 1.5-dva radius circular window around the central fixation point, while ~2.5 × 4 dva white bars swept in eight directions (four orientations) across the approximate location of the neuron's RF. Responses from the recording site were monitored audibly and visually by the experimenter, and the approximate boundaries of the RF were noted for the positioning of stimuli in subsequent behavioral tasks.

Visually Guided Saccade Task

Motion direction selectivity was measured during a visually guided saccade task (Figure 1A). Monkeys fixated within a 1.5-dva radius circular window around the central fixation point. After 500 msec of fixation, a moving grating appeared in the RF of the neuron being recorded. After 1000 msec (fixation period), the fixation point disappeared. On 50% of trials, a saccade target (1-dva black circle) appeared opposite the RF simultaneous with the offset of the fixation point; in this "away condition," the monkey saccaded away from the RF to the target to receive a reward (blue box in Figure 1A). On the remaining 50% of trials ("toward condition"), no target appeared and the monkey made a saccade to the moving grating to receive a reward (red box in Figure 1A). The fixation period was identical for the toward and away conditions. Gratings were 2.5-dva radius circles, 0.66 cycles/degree, with a drift speed of 7°/sec, and could move in eight different directions (45° increments) with full contrast, and four of those directions were presented with seven different contrasts (2–100%).

Experimental Design and Statistical Analysis

The perisaccadic window is defined as 65 msec before to 35 msec after the saccade onset; because the visual latency of MT neurons is typically ~40 msec, the response in this window will not be affected by a potential response to visual motion induced by the movement of the eye during the saccade. For comparison, the analysis of fixation period responses is based on the last 100 msec

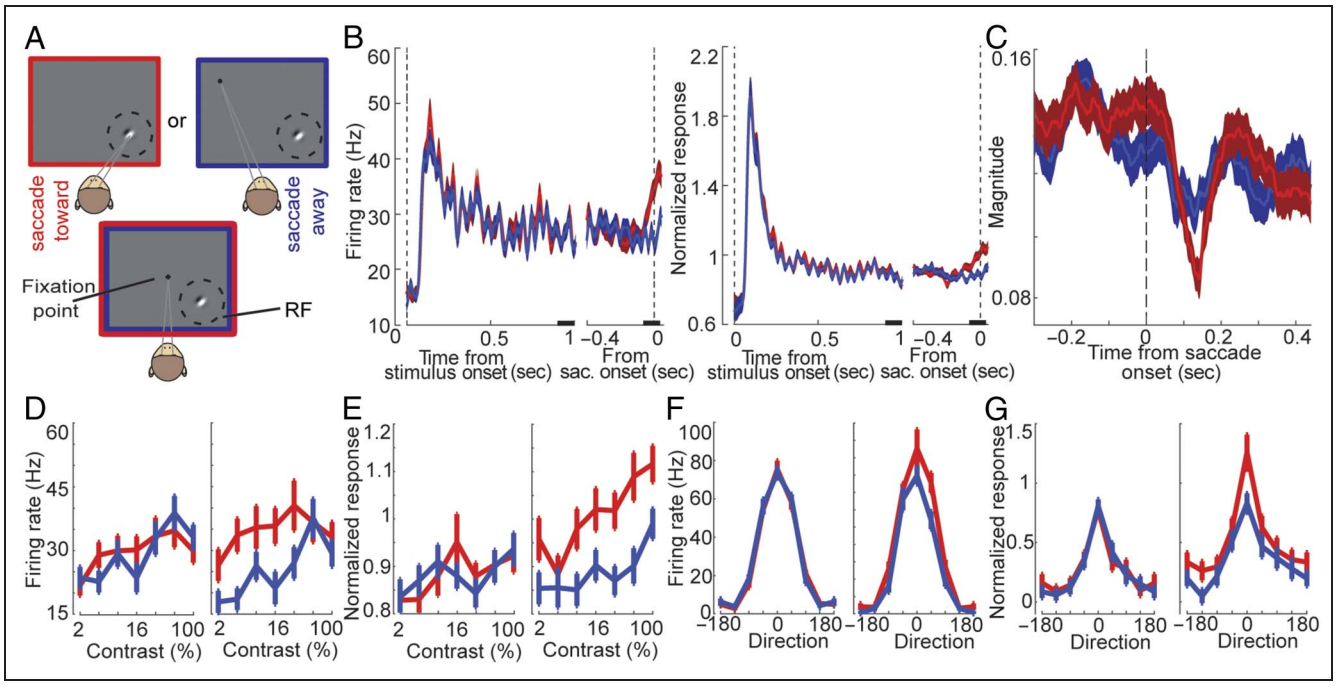

Figure 1. A saccade toward neurons' RFs enhances the neurons' perisaccadic FRs, contrast functions, and tuning curves. (A) In the visually guided saccade task, the monkey first fixated and a moving grating stimulus appeared in the neuron's RF. When the fixation point disappeared, the monkey made a saccade either to the grating stimulus (toward condition, red box), or to a target that appeared in the opposite visual hemifield (away condition, blue box). Plots in red and blue are for toward and away conditions, respectively in (B–G). (B) Left: PSTH of a sample MT neuron during presentation of visual stimulus for the toward and away conditions, aligned to the onset of the visual stimulus (left) or the saccade (right). Right: normalized PSTH of the population of MT neurons during presentation of visual stimulus for the toward and away conditions, aligned to the onset of the visual stimulus (left) or the saccade (right). PSTHs smoothed with a Gaussian of width 50 msec, plotted mean ± *SEM* over trials (left) or neurons (right). (C) Magnitude of the population response over time relative to the saccade, for the toward and away conditions (see Methods). Mean ± *SEM* in a sliding 100-msec bin. (D) The contrast function of the same sample MT neuron in fixation (left) and the perisaccadic period (right), for the toward and away conditions. (E) The normalized contrast function of the population of MT neurons, in fixation (left) and the perisaccadic period (right), for the toward and away conditions. (F) The direction tuning curve of the same sample MT neuron in fixation (left) and the perisaccadic period (right), for the toward and away conditions. (G) The normalized direction tuning curve of the population of MT neurons, aligned relative to their preferred direction at 0°, in fixation (left) and the perisaccadic period (right), for the toward and away conditions. Plots in (B–G) show mean ± *SEM*.

before the fixation point turns off (unless otherwise specified). Statistical comparisons were performed using the Wilcoxon sign-rank test, except where otherwise noted. Statistical tests are identified in the Results section for each of the experiments below.

Contrast Function

We obtained the contrast function of neurons by measuring the mean FR of neurons (pooled over different directions) for different contrasts during the fixation (Figure 1D, 1E left) and perisaccadic (Figure 1D, 1E right) periods. For the population contrast function, we normalized the contrast function of each neuron to the average response of the neuron across all contrasts and directions during the fixation period (1 sec).

Direction Tuning

We obtained the direction tuning of neurons by measuring the mean FR of neurons for different directions. First, we identified the preferred direction for each neuron based on its response to stimuli moving each direction at 100% contrast during the whole fixation period (1 sec). Tuning curves are plotted relative to that preferred direction (plotted at 0°), and based on the direction tuning of neurons during the 100-msec fixation (Figure 1F, 1G left) and perisaccadic periods in the toward or away conditions (Figure 1F, 1G right).

We normalized the direction tuning of each neuron (during the fixation and perisaccadic periods) using the following formula:

$$(\text{MEAN} - \text{MIN})/(\text{MAX} - \text{MIN})$$

where MEAN is the mean FR of each neuron to each stimulus direction during the fixation and perisaccadic periods, and MIN and MAX are the minimum and maximum responses of the same neuron across all stimulus directions over the entire 1-sec fixation period.

Reliability

We calculated FF as a measure of reliability. The FF was computed as the variance/mean of neuronal responses in a single condition across multiple trials. First, we studied the relationship between the different properties of visual stimuli (i.e., contrast and direction) and the reliability of neuronal responses during the fixation period. To do this, we slid a bin of 100 msec over the whole 1-sec visual period and calculated the FF across trials of the same type. To rule out differences in FRs as the cause of the observed correlation between stimulus contrast and changes in FF, we binned the mean FR of neurons throughout the fixation period (with a bin of 3 Hz) and recalculated the correlation coefficient between the variability of responses and the seven contrasts for each FR bin. To match the FRs between the toward and away conditions, we used the mean matching method developed by Churchland et al. (Churchland et al., 2010). This method involves looking at the FR for each neuron and time bin and discarding points until a common FR distribution between the two conditions is achieved. Rates were computed in a sliding 30-msec bin spanning the perisaccadic period.

Population Response Magnitude

To compute the magnitude of the population response in Figure 1C, we measured responses in a sliding bin of 100 msec, from 250 msec before to 400 msec after saccade onset. For each time point, we formed eight different polar vectors based on the responses of all neurons to the eight different motion directions and calculated the magnitude of the average response vector.

Correlated Activity

We calculated the correlated activity of responses of simultaneously recorded pairs of neurons during the fixation and perisaccadic periods (n = 271 pairs). In each case, the noise correlation was calculated over a 60-msec sliding window and then averaged across the period, using the Pearson correlation coefficient across trials. To match the FR between different conditions, we used the method developed by Churchland et al. (Churchland et al., 2010).

Discriminability

To measure the ability of the population response to discriminate between two conditions, we applied a method similar to that used in the work of Cohen and Maunsell (2009; Figure 5). Each point in Figure 5A represents the mean FR of simultaneously recorded neuronal pairs for each trial in response to two different categories of stimulus. Then, we projected each point onto the imaginary line that connects the centers of the two categories' clusters (centers are shown by gray crosses in Figure 5A). Finally, we measured the discrimination between the two different projected distributions related to the two different categories. To measure the discrimination between the two distributions, we employed the d' index, defined as:

$$d' = \frac{\mu_1 - \mu_2}{\sqrt{\frac{\delta_1^2 + \delta_2^2}{2}}}$$

where μ_i and δ_i are the average and standard deviations of projected points related to the ith category.

Contribution to Change in Discriminability

To determine how the observed neuronal modulations of FR, reliability, and correlated activity of MT responses contribute to changes in discriminability during the perisaccadic period, we used a model first developed by Shadlen, Britten, Newsome, and Movshon (1996) to generate

artificial trials with the desired FR, FF, and noise correlation. This model was also used to measure the contribution of three different factors—FR, reliability, and correlated activity of neuronal responses—to attentional improvement of V4 population sensitivity (Cohen & Maunsell, 2009).

The model is formulated as:

$$x = m + yv$$

where m and v are respectively the $n \times 1$ vectors of the mean and variance of activities from n simultaneously recorded neurons, and Y is calculated as in:

$$Y = qz$$

where z is a $n \times 1$ normally distributed zero-mean random vector with unit variance and q is the square root of the $n \times n$ correlation matrix r (i.e., $r = q'q$). The correlation matrix r incorporates the interneuron correlation values calculated from the responses of every possible combination of neuronal pairs. Finally, x provided the simulated responses for n units, which resembled the experimentally measured responses of n simultaneously recorded neurons.

To determine the contribution of each factor (i.e., gain [G], reliability [R], and correlated activity [CA]) to the enhanced discriminability during the perisaccadic period, we generated the artificial data based on the value of one factor in the toward condition (i.e., G+, R+, and CA+), and the values of the other two factors in the away condition (i.e., G−, R−, and CA−; Figure 6A). Then, we used the method explained in Figure 5A to calculate the discrimination between two different categories (e.g., two different saccade directions, stimulus contrasts, or motion directions) for the generated artificial data, giving us a discrimination value for each factor (gain, reliability, correlated activity) for each information category (saccade direction, contrast, motion direction). The proportion of the discrimination value for each factor alone to the discrimination value for all the factors together determined the contribution of that factor to that category of information. For the contrast and direction calculations, d' values for all contrast and direction pairs were averaged.

RESULTS

Perisaccadic Enhancement and Saccadic Suppression

We recorded the activity of 84 MT neurons during a visually guided saccade task (82 with 16-channel linear array electrodes and two with single electrodes; Figure 1A). The stimulus was always placed at and around the RF of the MT neurons, enabling us to study the influence of overt attention on the part of the visual representation involved in processing the target of attention. Figure 1B (left) shows the response of a sample MT neuron during the task. During the fixation period, there was no significant difference in the FR of the neuron between the toward and away conditions (FR_{toward} = 26.566 ± 0.126 Hz, n = 445; FR_{away} = 26.157 ± 0.124 Hz, p = .661, Wilcoxon rank-sum test). However, during the perisaccadic period, there was a significant increase in the FR of the neuron for the toward condition compared to the away condition (FR_{toward} = 35.065 ± 0.164 Hz, n = 445; FR_{away} = 26.423 ± 0.131 Hz, n = 483, p = .001, Wilcoxon rank-sum test); we refer to changes in FR as "gain," without attempting to differentiate between additive versus multiplicative modulation of the FR. A similar increase in perisaccadic response gain was evident in the population of MT neurons (Figure 1B, right). There was no significant FR difference between the toward and away conditions during the fixation period, but the same population of MT neurons showed a significant perisaccadic modulation of their FR (fixation: $\Delta FR_{toward–away}$ = −0.006 ± 0.108 Hz, p = .727; perisaccadic: $\Delta FR_{toward–away}$ = 1.133 ± 0.245 Hz, p < .001); this difference between the toward and away conditions was driven by a perisaccadic increase in the FR in the toward condition, compared to 200–300 msec before saccade onset (ΔFR_{toward} = 1.172 ± 0.256 Hz, p < .001, n = 84), with no perisaccadic change in the FR for the away condition (ΔFR_{away} = −0.051 ± 0.137 Hz, p = .292, n = 84). In summary, MT neurons enhance their response gain when a saccade is directed toward their RF, resembling the phenomenon previously reported in other extrastriate areas (Steinmetz & Moore, 2010, 2014; Sheinberg & Logothetis, 2001).

Previous reports show suppression of MT responses shortly after the onset of saccades (Bremmer, Kubischik, Hoffmann, & Krekelberg, 2009; Thiele, Henning, Kubischik, & Hoffmann, 2002), which is thought to be important for suppressing the induced motion signal because of high-velocity eye movements. Consistent with this, we observed a decrease in the MT population response following saccade onset. For each time point (100-msec sliding bin), first we formed eight different polar vectors based on the responses of neurons to eight different motion directions and then calculated the magnitude of the average response vector. Figure 1C shows the magnitude of the average response vector around saccade onset; the magnitude of the average response vector for saccades in either direction decreases significantly from 100 to 200 msec after saccade onset compared to 200–100 msec before saccade onset (toward: $\Delta magnitude_{post\text{-}pre}$ = −0.037 ± 0.007, n = 84, p < .001; away: $\Delta magnitude_{post\text{-}pre}$ = −0.028 ± 0.006, n = 84, p < .001). Note that this suppression occurs later relative to the saccade onset than the increases in FR for the toward condition. The remainder of our analysis will focus on the perisaccadic period in which enhanced FRs are observed, before the onset of saccadic suppression effects.

Perisaccadic Contrast Functions and Tuning Curves

Eye movements are associated with an enhancement of saccade target representations, in terms of feature

discrimination (Rolfs & Carrasco, 2012; Deubel & Schneider, 1996) and contrast threshold (Rolfs & Carrasco, 2012). In order to gain insight into the neural basis of improved contrast detection thresholds during saccades, we assessed perisaccadic changes in the contrast response functions. Visual stimuli ranged from 2% to 100% contrast. We obtained the contrast function of neurons by measuring the mean FR of neurons (pooled across directions) for different contrasts. The contrast response function of the same example neuron shown in Figure 1B is plotted in Figure 1D. On the left are the contrast response functions measured during fixation, with no significant difference between the toward and away conditions (two-way ANOVA, effect of Saccade Direction, $F = 0.040$, $p = .847$; effect of Contrast, $F = 2.550$, $p = .018$; interaction, $F = 1.110$, $p = .352$). The right-hand plot shows the same neuron's contrast response functions during the perisaccadic period. Preparing a saccade toward the neuron's RF increased the neuron's responses across a range of contrasts (two-way ANOVA, effect of Saccade Direction; $F = 17.930$, $p < .001$; effect of Contrast, $F = 2.790$, $p = .011$; interaction, $F = 1.180$, $p = .313$). Figure 1E shows a similar perisaccadic shift in the contrast response function for the population of MT neurons. During fixation, the population of MT neurons did not show significantly different responses to various contrasts between the toward and away conditions; however, during the perisaccadic period, their contrast response function was significantly different between the two conditions (fixation: two-way ANOVA, effect of Saccade Direction, $F = 0.020$, $p = .881$, effect of Contrast, $F = 2.030$, $p = .059$, interaction, $F = 0.59$, $p = .739$; perisaccadic: two-way ANOVA, effect of Saccade Direction, $F = 33.620$, $p < .001$, effect of Contrast, $F = 5.010$, $p < .001$, interaction, $F = 0.790$, $p = .581$).

Changes in the feature tuning of individual neurons can also impact the population representation (Montemurro & Panzeri, 2006; Seriès, Latham, & Pouget, 2004). We examined the effect of saccade preparation on neural tuning by measuring the mean FR of neurons for different stimulus motion directions during the perisaccadic and visual periods. The neuron's preferred direction and direction tuning was defined based on its response to stimuli at 100% contrast during the whole fixation period (1 sec). Figure 1F left shows the direction tuning of the sample MT neuron in the fixation period, which was not significantly different between the toward and away conditions (two-way ANOVA, effect of Saccade Direction, $F = 0.070$, $p = .797$). However, during the perisaccadic period, saccading toward the neuron's RF significantly increased the neuron's response (two-way ANOVA, effect of Saccade Direction, $F = 16.050$, $p < .001$, Figure 1F right). Figure 1G shows the normalized direction tuning of the population of MT neurons, during the visual (left) and perisaccadic (right) periods (see Methods for normalization procedures). The population of MT neurons did not show a significant difference between their tuning curves for the toward versus away condition during the fixation period (two-way ANOVA, effect of Saccade Direction, $F = 0.020$, $p = .902$). In this time period, there was no significant difference between neurons' responses during the toward and away conditions, either for their preferred (normalized $\Delta FR_{toward-away} = -0.029 \pm 0.070$, $p = .964$) or nonpreferred direction stimulus (normalized $\Delta FR_{toward-away} = 0.073 \pm 0.090$, $p = .406$). During the perisaccadic period, in contrast, responses were significantly higher for the toward condition (two-way ANOVA, effect of Saccade Direction, $F = 12.610$, $p < .001$). This increase in FR in the toward condition was significant for the preferred stimulus direction (normalized $\Delta FR_{toward-away} = 0.428 \pm 0.158$, $p = .033$), but not for the nonpreferred direction (normalized $\Delta FR_{toward-away} = 0.138 \pm 0.084$, $p = .081$). This increase in FR was also significant when considering a shorter window ending at saccade onset ($\Delta FR_{toward-away} = 1.186 \pm 0.216$ Hz, $n = 84$, $p < .001$). This gain-like increase in FR when saccading toward a stimulus in the neuron's RF has the potential to improve population encoding of stimulus direction.

Neuronal Variability Reflects Stimulus Contrast and Drops Perisaccadically

Previous studies have reported a perisaccadic drop in the variability of neurons' responses (Steinmetz & Moore, 2010), but have not looked for an interaction between this change in variability and stimulus properties, which have been shown to influence variability in MT (Ponce-Alvarez, Thiele, Albright, Stoner, & Deco, 2013). As a measure of variability, we calculated the FF, the ratio of the variance to the mean of neuronal responses in a single condition across multiple trials. First, we studied the relationship between the different properties of visual stimuli (i.e., contrast and direction) and the variability of neuronal responses during the visual period. Figure 2A shows the average value of the FF during the fixation period in response to different contrasts. The onset of the visual stimulus is followed by a reduction in response variability of the sample neuron, consistent with the previous literature (Churchland et al., 2010). The FF is more reduced as the contrast of the stimulus increases (light to dark gray plots represent low to high contrast stimuli, respectively). The scatter plot in Figure 2B shows the mean value of the FF over the visual period for seven contrasts (averaged across motion directions), indicating a negative correlation between the variability of the response and the contrast of the stimulus ($r = -.924$, $p = .003$, Pearson correlation coefficient). Considering the nonlinear relationship between the FR and FF, we also assessed the relationship between contrast and FF when FR is kept similar across stimuli (see Methods). Gray dots in the scatter plot in Figure 2B indicate the rate-matched variability (FR range = 16–19 Hz), showing a negative correlation between FF and contrast for this

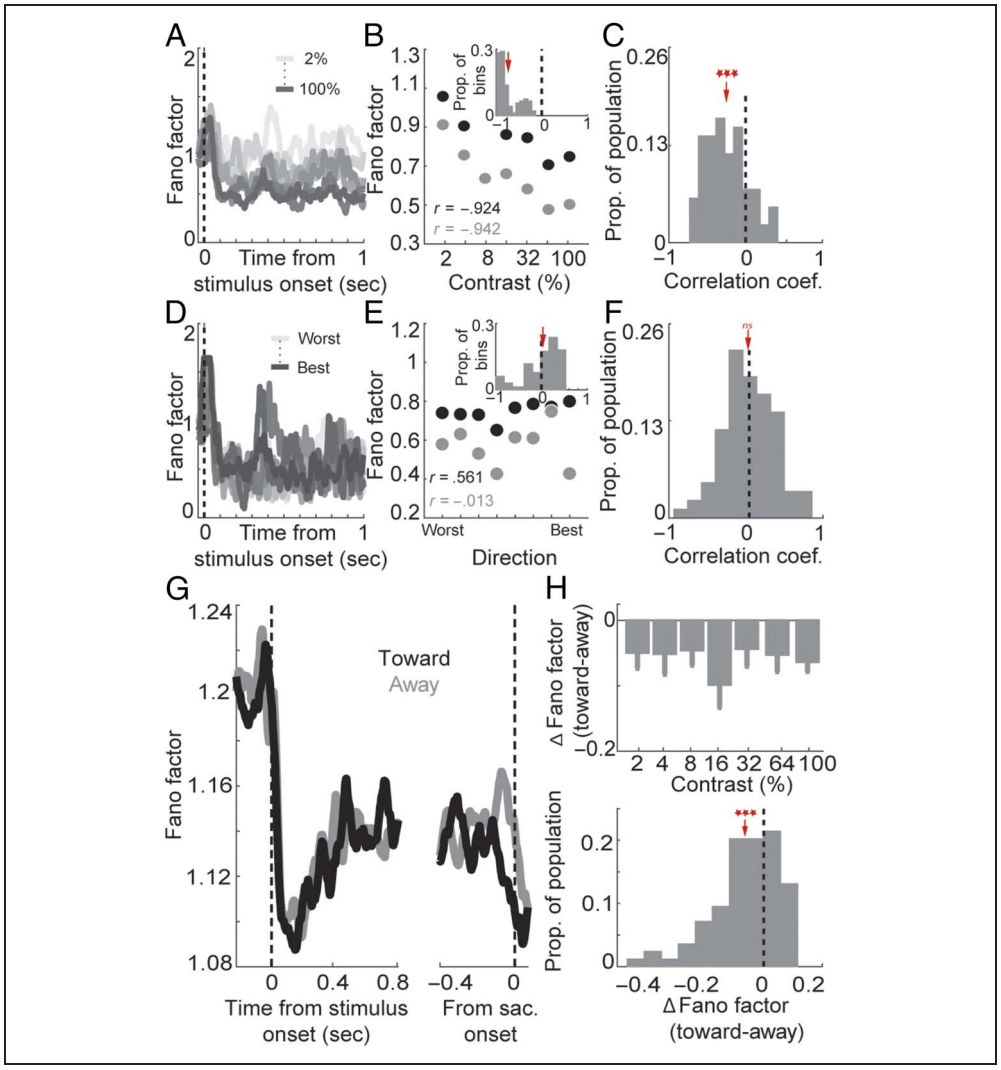

Figure 2. Neuronal variability is modulated by stimulus contrast and saccade direction. (A) FF of a sample MT neuron for seven different contrasts (shades of gray) during the visual period. (B) Scatter plot shows mean FF of the same sample neuron for each of seven contrasts, for all data (black dots), and for the bin of 16–19 Hz (gray dots). The inset histogram shows the distribution of the correlation coefficient values when rate-matching in each possible 3-Hz wide FR bin. The mean value of this distribution is one value in the population histogram in (C), which shows the mean correlation coefficient of the FF and the contrasts of stimuli across different FR bins for the population of MT neurons. (D) FF of the same sample MT neuron in response to eight different directions of motion (worst [light gray] to best [dark gray]) during the visual period. There was no relationship between the reduction in FF following stimulus onset and the stimulus direction of motion. (E) Scatter plot shows the mean value of the FF of the same sample neuron during the visual period for directions of motion (sorted worst to best), for all data (black dots) or in a rate-matched bin of 16–19 Hz (gray dots). The inset histogram shows the distribution of the values of the correlation coefficient between FF and motion direction when rate-matching in each possible 3-Hz wide FR bin. The mean value of this distribution is one value in the population histogram in (F), which shows the mean correlation coefficient of the FF and the motion direction of stimuli across different FR bins for the population of MT neurons. (G) FF over time, aligned to the stimulus onset (left) and saccade onset (right), for the toward (black) and away (gray) conditions. (H) Top: Bar plot shows the population perisaccadic difference in FF (toward–away) for each of the seven contrast levels, mean ± *SEM*. Bottom: Histogram shows the difference in FF (toward–away) during the perisaccadic period, for the population of MT neurons (each neuron and contrast level considered separately). ***$p < .001$; *ns* = not significant.

sample FR range ($r = -.942, p = .002$, Pearson correlation coefficient). The distribution of the measured correlation coefficients across different FR ranges is shown in the inset histogram, indicating that, as the contrast of the stimulus increases, the variability of this sample neuron decreases, independent of the neuron's FR. We measured the average correlation across various FR ranges for each individual neuron. Figure 2C shows the distribution of the correlation values for the population of MT neurons; across the population, the response variability significantly decreases as the contrast of the stimulus increases (correlation coefficient = $-0.243 \pm 0.030, p < .001$). Figure 2D shows the variability of the sample MT neuron in response to 100% contrast stimuli measured separately for eight different directions during the fixation period (light to dark gray plots represent the worst to best direction, respectively). There was no apparent relationship between the magnitude of the FF reduction after stimulus onset and the direction of the stimulus. The black dots in the scatter plot in Figure 2E are the mean value of FF over the fixation period for eight directions. We did not find a significant correlation between the variability of the response and the stimulus direction ($r = .561, p = 0.148$, Pearson correlation coefficient). Similar to the analysis in Figure 2B–2C, we rate-matched the FF and recalculated the correlation coefficient between the FF and different directions. Figure 2E shows FF as a function of motion direction, for the 16- to 19-Hz range (gray), demonstrating no significant correlation between the FF values and the directions of stimuli ($r = -.013, p = .975$, Pearson correlation coefficient). The inset histogram in Figure 2E shows the distribution of the correlation coefficient values

for various FR ranges for the sample neuron, and Figure 2F shows the distribution of average correlations across population (correlation coefficient = $-.006 \pm 0.035$, $p = .918$). These results show that contrast, but not motion direction, affects the magnitude of FF reduction with stimulus onset.

Knowing the relationship between the FF and stimulus contrast and motion direction, we sought to study the influence of overt attention on perisaccadic changes in FF (Steinmetz & Moore, 2010). Figure 2G shows the time course of the average FF in the toward and away conditions. Figure 2H (top) shows the mean difference in the response variability (toward–away) for the population of MT neurons across different contrasts, indicating that there is no significant relationship between the FF reduction and stimulus contrast (two-way ANOVA, effect of Saccade Direction, $F = 14.741$, $p < .001$; effect of Contrast, $F = 0.801$, $p = .566$; interaction, $F = 0.231$, $p = .966$). Figure 2H (bottom) shows the distribution of differences in the response variability (toward–away, all contrasts) for the population of MT neurons during the perisaccadic period. Preparing a saccade toward neurons' RFs significantly reduces the variability of neuronal responses compared to a saccade in the opposite direction ($\Delta FF_{toward-away} = -0.062 \pm 0.013$, $p < .001$). This decrease in variability was also significant when considering a shorter window ending at saccade onset ($\Delta FF_{toward-away} = -0.054 \pm 0.017$ Hz, $n = 84$, $p < .001$). To summarize, we found that the stimulus contrast, but not its motion direction, influences the reliability of visual signaling in MT, and this reliability is enhanced by impending eye movements toward the neuron's RF, independent of stimulus contrast.

Comparison of Upper versus Lower Visual Hemifields

It has previously been reported that saccades to the upper visual hemifield have faster latencies than those to the lower visual hemifield (Hafed & Chen, 2016). We confirmed this phenomenon in our data set: Figure 3A shows the monkeys' RTs for saccades to stimuli in different ranges of Y coordinates (nine upper hemifield, 75 lower hemifield). RTs for saccades to the upper visual field were faster than those to the lower field ($\Delta RT_{upper-lower} = -31.400 \pm 2.416$ msec, $n = 32$, $p < .001$). Despite this difference in RT, the perisaccadic FR and FF changes were not significantly different between the upper and lower visual fields (upper: $\Delta FR_{toward-away} = 1.240 \pm 0.570$ Hz, $n = 9$; lower: $\Delta FR_{toward-away} = 1.120 \pm 0.267$ Hz, $n = 75$, $p = .479$, Wilcoxon rank-sum test; upper: $\Delta FF_{toward-away} = -0.029 \pm 0.031$, $n = 9$; lower: $\Delta FF_{toward-away} = -0.066 \pm 0.014$, $n = 75$, $p = .418$, Wilcoxon rank-sum test; Figure 3B and 3C).

Perisaccadic Decorrelation of MT Responses

Representation of visual stimuli at the level of the population depends on correlated activity between neurons (Merrikhi, Clark, & Noudoost, 2018; Kohn, Coen-Cagli, Kanitscheider, & Pouget, 2016; Hu, Zylberberg, & Shea-Brown, 2014; Ecker, Berens, Tolias, & Bethge, 2011). In order to determine whether overt attention influences the structure of these correlations, we calculated the correlated variability of responses of simultaneously recorded pairs of neurons during the fixation and perisaccadic periods ($n = 271$ pairs). In each case, the noise correlation was calculated over a 60-msec sliding window and then averaged across the period, using the Pearson correlation coefficient across trials; FRs between different conditions were rate-matched (see Methods). Interestingly, across the whole population, the correlated activity of neuronal responses during the perisaccadic period did not significantly differ based on the location of the upcoming saccade or the stimulus contrast (two-way ANOVA, effect of Saccade Direction, $F = 1.110$, $p = .292$; effect of Contrast, $F = 1.240$, $p = .283$; interaction, $F = 0.691$, $p = .660$). However, when we divided the population of neurons based on their baseline correlation (measured during the 1-sec fixation period), we found that the magnitude of correlations dropped during the perisaccadic period (i.e., responses were decorrelated). Figure 4A shows the correlated variability of three sample pairs of neurons, aligned to the onset of stimulus (left) or saccade (right), during the toward condition. For the sample pair with a positive

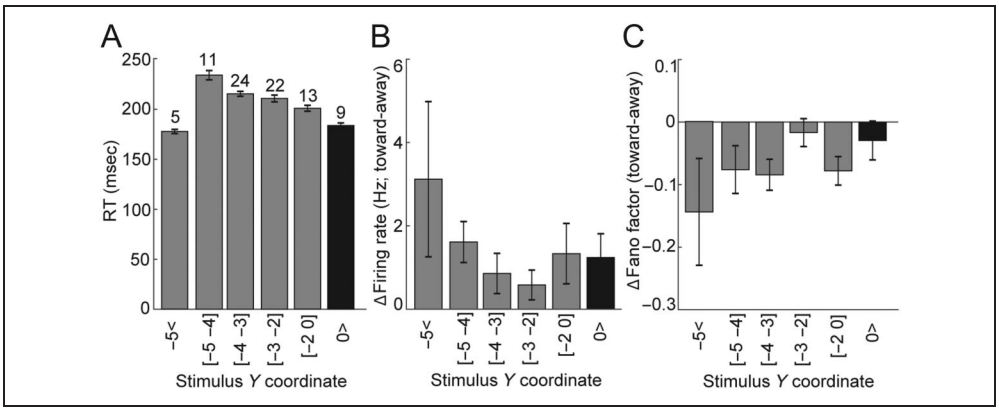

Figure 3. RT, FR, and FF as a function of distance from horizontal meridian. (A) RT for saccades to RFs at various y axis positions (indicated bottom). Saccades to the upper visual hemifield (y-position 0–8.5 dva) had faster RTs. Numbers at top indicate the number of neurons in each group, bars show mean ± *SE*. (B) Change in FR (toward–away) for neurons with RFs at various y axis positions. (C) Change in FF (toward–away) for neurons with RFs at various y axis positions.

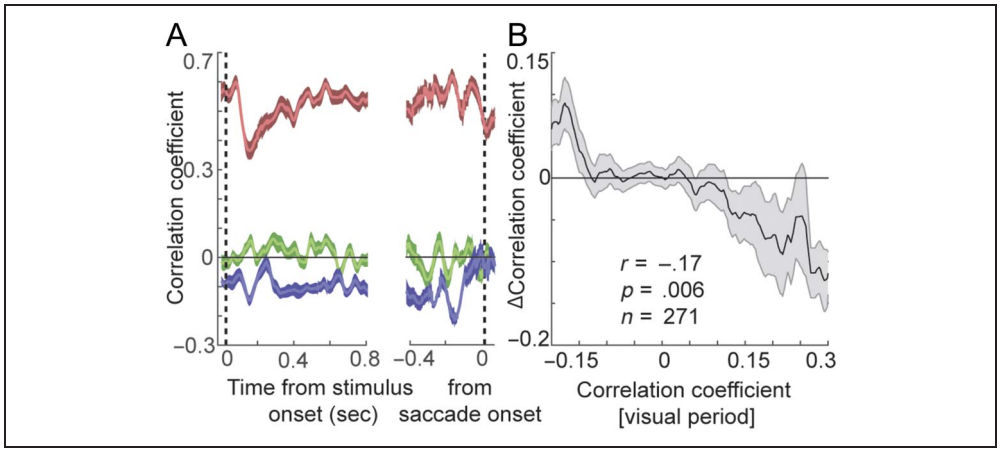

Figure 4. Saccade preparation decorrelates MT responses. (A) The correlated variability of three sample pairs' responses during the toward condition, aligned to the onset of the stimulus (left) or the saccade (right). Sample pairs with positive (red), near-zero (green), or negative (blue) correlations during the visual period experienced a perisaccadic decrease, no change, or increase in noise correlation (toward vs. away), respectively. (B) The difference between the perisaccadic noise correlations of MT neuronal pairs in the toward and away conditions, as a function of their noise correlation during the visual period. All plots mean ± *SEM*.

baseline noise correlation, preparing a saccade toward the neurons' RFs reduced the correlated activity compared to a saccade in the opposite direction (red, Δcorrelation coefficient$_{toward–away}$=−.100 ± .040, n = 32, p = .120). The correlated activity of the responses of a sample pair with a small noise correlation (close to zero) during the fixation period did not change based on upcoming saccade direction during the perisaccadic period (green, Δcorrelation coefficient$_{toward–away}$ = −.060 ± .040, n = 32, p = .750). However, for the sample pair with a negative baseline noise correlation, preparing a saccade toward neurons' RFs reduced the magnitude of the negative correlation (blue, Δcorrelation coefficient$_{toward–away}$ = .130 ± .040, n = 32, p = .038). We found that, across the population, the saccade-induced change in the noise correlation (toward–away) decreases as the correlated activity of neuronal pairs during the fixation period increases (r = −.170, n = 271, p = .006, Pearson correlation coefficient; Figure 4B). We also confirmed that after exclusion of pairs recorded from neighboring recording contacts, the relationship between the saccade-induced change of noise correlation and the pairs' correlation during fixation is still statistically significant (r = −.164, n = 258, p = .009, Pearson correlation coefficient). Therefore, an impending saccade toward the neurons' RFs generally decorrelated neuronal responses, compared to a saccade to the opposite hemifield.

Perisaccadic Changes Enhance Visual and Motor Information

Having seen that overt attention alters neurons' response reliability and correlated activity, we examined how these neuronal changes relate to the enhanced representation of saccade targets. We first verified that saccades toward the RF enhance the population-level representation of the saccade direction, visual motion direction, and contrast. As shown in Figure 5A, we can assess the ability of the population to discriminate a specific aspect as the d' measured by the joint responses of two neurons in two different conditions (e.g., two different motion directions when assessing the motion discriminability). Figure 5B shows that, during the perisaccadic period, the motion discriminability was significantly greater for saccades toward the neurons' RFs compared to saccades away (Δmotion discriminability = 0.051 ± 0.011, n = 271, p < .001). Similarly, the population was significantly better able to discriminate between contrasts for toward compared to away conditions during the perisaccadic period (Figure 5C; Δcontrast discriminability = 0.027 ± 0.007, n = 271, p < .001). The ability to discriminate toward versus away conditions themselves (saccade direction discriminability) was significantly greater than zero (saccade direction discriminability: $d'_{\text{toward vs. away}}$ = 0.157 ± 0.012, n = 271, p < .001; Figure 5D). Therefore, directing overt attention to MT neurons' RFs enhanced their capacity to represent saccades, contrast, and motion direction.

Contribution of Response Changes to the Perisaccadic Representation

After confirming that the representation of saccade direction, stimulus contrast, and motion are all enhanced perisaccadically, we set out to quantify the contribution of each of the neuronal response changes to these perisaccadic representational enhancements. To evaluate the contribution of each change independently, we first used a model to generate multiple artificial data sets, each reflecting only one of the perisaccadic changes observed in the actual data (Figure 6A, Methods; Shadlen et al., 1996). Although in the data changes in noise correlations could also contribute to changes in variability, here, we test their contributions separately using model-generated data in which independent variability alone accounts for the change in the FF, and changes

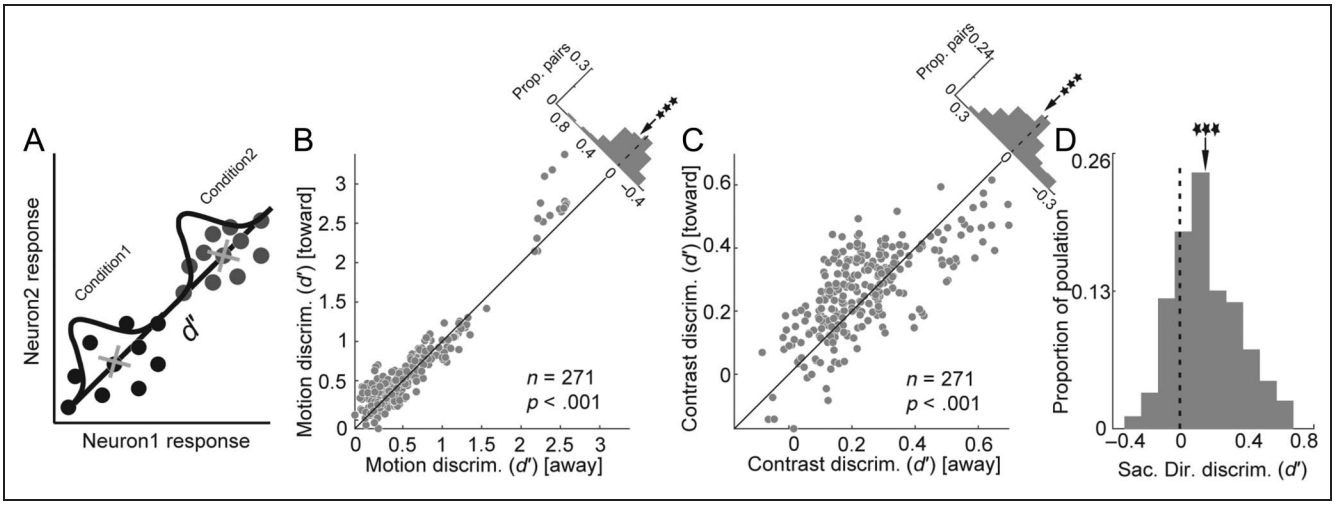

Figure 5. Perisaccadic representational enhancement of MT neuronal responses. (A) Schematic illustrating discriminability calculation. Each point, which represents the mean FR of neuronal pairs in response to two different categories, was projected onto the imaginary line between two clusters. The discrimination between two different projected distributions was calculated using the d' index. (B) Discriminability between motion directions for saccades toward versus away from RF, for pairs of MT neurons and directions. (C) Discriminability between contrasts for saccades toward versus away from RF, for pairs of MT neurons and contrasts. Histograms in (B–C) show distributions of difference (toward–away). (D) Histogram shows the discriminability between toward versus away conditions (motor discriminability).

in noise correlations do not impact the FF. To calculate the contribution of each type of response change, we evaluated the perisaccadic discriminability (d' for motion direction, contrast, or saccade direction; Figure 6B; averaged across all pairs of conditions for contrast and direction) when each of the changes (gain, reliability, and correlated activity) occurred in isolation—that is, using the model to generate data in which only one of these variables matched the value observed in the "toward" condition, and the rest matched their values in the "away" condition (see Methods). We found that different aspects of the perisaccadic response modulation contributed to the representation of the motor plan (saccade direction) versus visual information (contrast and direction). The improved encoding of upcoming saccade direction in the MT responses was based almost entirely on the change in gain, with minimal influence of changes in reliability or correlated activity (Figure 6C; saccade direction discrimination: $d'_{\text{gain}} = 0.289 \pm 0.017$, $n = 266$, $p < .001$; $d'_{\text{reliability}} = 0.002 \pm 0.0003$, $n = 266$, $p < .001$; $d'_{\text{correlated activity}} = -0.002 \pm 0.0006$, $n = 266$, $p < .001$). In contrast, the increase in visual information for saccade targets (either motion direction or contrast) drastically benefited from the changes in reliability and correlated activity. When discriminating between contrasts, changes in gain, reliability, and correlated activity all contributed to the enhanced perisaccadic population representation (Figure 6D–6E; contrast discrimination: $d'_{\text{gain}} = 0.314 \pm 0.015$, $n = 246$, $p < .001$; $d'_{\text{reliability}} = 0.275 \pm 0.017$, $n = 246$, $p < .001$; $d22_{\text{correlated activity}} = 0.265 \pm 0.013$, $n = 246$, $p < .001$; motion direction discrimination: $d'_{\text{gain}} = 0.724 \pm 0.041$, $n = 255$, $p < .001$; $d'_{\text{reliability}} = 0.622 \pm 0.036$, $n = 255$, $p < .001$; $d'_{\text{correlated activity}} = 0.645 \pm 0.039$, $n = 255$, $p < .001$).

Overall, assessing the contribution of each aspect of the change in perisaccadic responses to the enhanced representation of saccade targets, we found a unique contribution of reliability and correlated activity in contrast and motion information processing, but not in the encoding of saccade direction (Figure 6F; contributions in saccade direction: gain = 99.170%, reliability = 1.160, correlated activity = −0.340%; contributions in contrast discrimination: gain = 36.910%, reliability = 32.150, correlated activity = 30.930%; contributions in motion discrimination: gain = 36.690%, reliability = 31.090%, correlated activity = 32.210%). These results provide insight into the role of changes in various aspects of network activity in the representational enhancement of saccade targets. For example, one can argue that the changes in the magnitude of response employ an external gain modulator to alter the gain, whereas changes in the response variability (either dependent correlated activity or reliability) might recruit changes within the network. Figure 6G contrasts the gain contributions versus variability contributions to various aspects of the saccade target representation. For feature information (contrast and motion), variability's contribution is greater than gain ($\Delta d'_{\text{contrast}} = -0.226 \pm 0.024$, $n = 246$, $p < .001$; $\Delta d'_{\text{motion}} = -0.544 \pm 0.043$, $n = 255$, $p < .001$). The motor information, however, is primarily dependent on the gain of visual signals ($\Delta d'_{\text{motor}} = 0.290 \pm 0.017$, $n = 266$, $p < .001$). These results clearly show the significance of changing the response variability in feature enhancement; however, it should be noted that the changes at the level of individual neurons still play a larger role compared to those at the population level. Gain and reliability are factors affecting individual neurons. We contrasted the contributions of the sum of

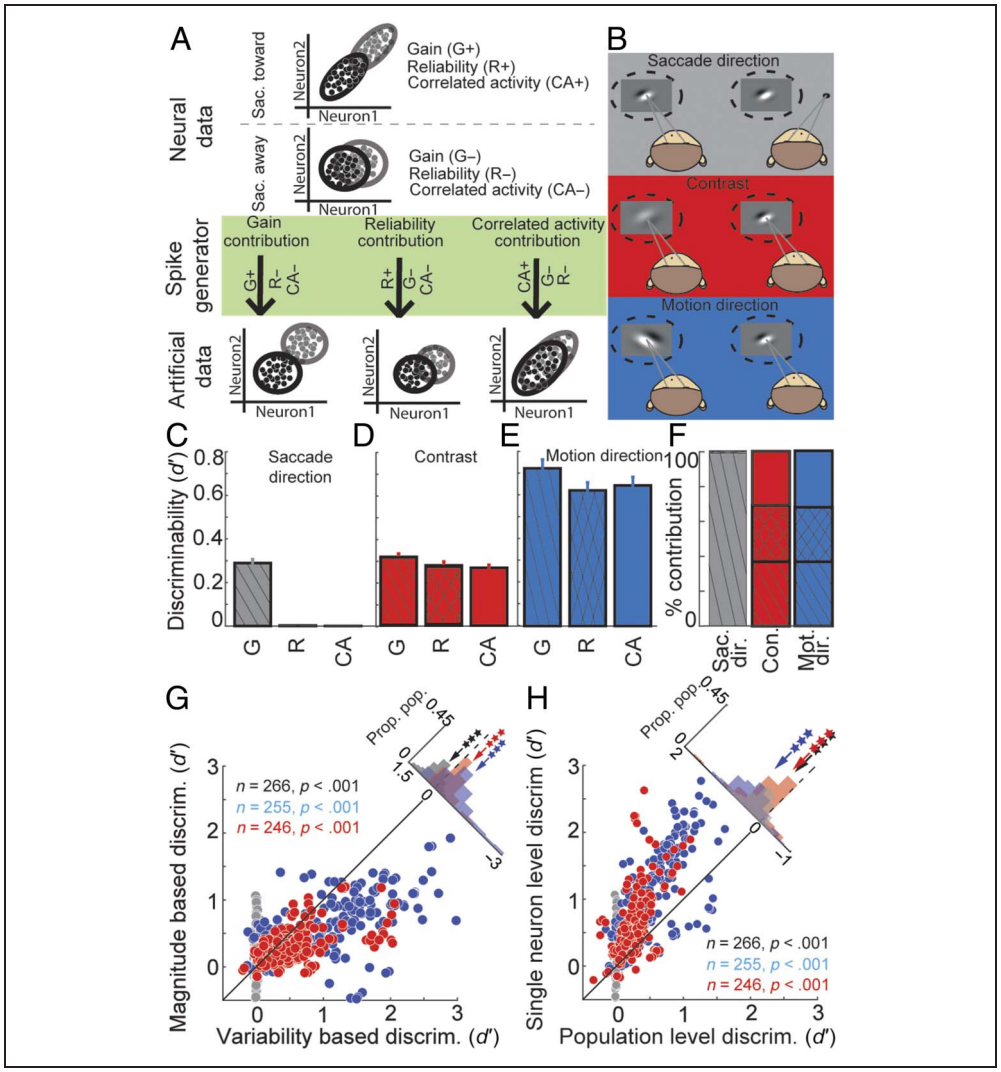

Figure 6. The contribution of gain, reliability, and correlated activity to the perisaccadic representation of saccade targets. (A) Schematic illustration of how artificially generated data was used to isolate the contributions of gain, correlated activity, and reliability to perisaccadic discriminability. Top: The FRs from each pair of simultaneously recorded neurons (illustrated schematically on the left) provided experimental values for gain (G), reliability (R), and correlated activity (CA) in the saccade toward (top: G+, R+, CA+) and away (bottom: G−, R−, CA−) conditions. Middle: A spike generator model was used to generate artificial data in which one factor (G, R, or CA) matched the value observed in the toward condition (+ symbol), and the other two factors' values matched those observed in the away condition (− symbol). The data in which the gain value matched the toward condition was used to measure the gain contribution (left: G+, R−, CA−; and analogously for reliability, middle, and correlated activity, right). Bottom: schematic illustration of artificial data generated for the same neuron pair, in which the value of one factor (G, R, or CA) matches that from the toward condition, and the other two match that of the away condition. This artificial data will be used to measure the perisaccadic discriminability when only one factor (G, R, or CA) has the value observed in the toward condition. (B) Perisaccadic discriminability (d') was calculated between saccade directions (top, gray), contrasts (middle, red), and motion directions (bottom, blue). (C–E) Perisaccadic discriminability based on the saccade toward value of only the gain, reliability, or correlated activity, for saccade direction (C), contrast (D), and motion direction (E), calculated using the artificially generated data. Contrast and motion direction discriminability were averaged across all pairs of conditions. Mean ± *SEM* across neural pairs. (F) Comparison of percentage of contribution of each factor (indicated by texture) to saccade direction (gray), contrast (red), and motion direction (blue). The ratio of d' for each factor alone compared to all three in combination was used to calculate the percentage contribution. (G) The perisaccadic discriminability for saccade direction (gray), contrast (red), and motion direction (blue), calculated using perisaccadic gain versus perisaccadic variability (reliability and correlated activity). (H) The perisaccadic discriminability for saccade direction (gray), contrast (red), and motion direction (blue), calculated using single-neuron variables (gain and reliability) versus population variables (correlated activity). Each dot in the scatter plots in (G and H) indicates d' for one neuronal pair. Histograms in the upper right show the distribution of differences across pairs.

these two factors versus the correlated activity of neurons, which only affects the population representation (Figure 6H). Population-level information for motion and contrast are significantly above zero, indicating the presence of such information beyond individual neuronal response changes ($d'_{\text{motion}} = 0.646 \pm 0.038$, $n = 255$, $p < .001$, $d'_{\text{contrast}} = 0.265 \pm 0.013$, $n = 246$, $p < .001$). Motor information was not greater than zero at the level of the population ($d'_{\text{motor}} = -0.002 \pm 0.001$, $n = 266$, $p < .001$). However, in all those aspects information at the level of individual neurons exceeded the population-level information ($\Delta d'_{\text{motor}} = 0.294 \pm 0.017$, $n = 266$, $p < .001$; $\Delta d'_{\text{contrast}} = 0.326 \pm 0.024$, $n = 246$, $p < .001$; $\Delta d'_{\text{motion}} = 0.535 \pm 0.027$, $n = 255$, $p < .001$).

DISCUSSION

In order to understand how changes in the visual representation enhance our perception of saccadic targets, we studied changes in the responses of MT neurons around the time of saccades. We found that just before a saccade into the neurons' RFs, the gain of neuronal responses to visual stimuli in the RF increased. The reliability of individual neural responses also increased. The effect of an

upcoming eye movement on the correlations between neurons was to decorrelate their responses compared to the visual period: An impending saccade toward the neurons' RFs reduced the magnitude of both positive and negative correlations. Thus, directing overt attention to the neuron's RF enhanced the response gain and reliability and changed the correlated activity of neurons. Prior work has shown that both overt and covert attention increase the magnitude (Moore et al., 1998; Treue & Maunsell, 1996; Moran & Desimone, 1985; Fischer & Boch, 1981) and feature discriminability (Moore & Chang, 2009; Chelazzi, Miller, Duncan, & Desimone, 2001; McAdams & Maunsell, 1999; Moore, 1999; Spitzer, Desimone, & Moran, 1988) of visually evoked responses, while decreasing trial-to-trial variability (Steinmetz & Moore, 2010; Cohen & Maunsell, 2009; Mitchell, Sundberg, & Reynolds, 2007). The majority of the previous overt attention studies were conducted in V4, and the current results extend these findings on overt attentional modulation to the dorsal visual stream. During covert attention, V4 neurons increase their sensitivity through a contrast gain increase, in which the largest increases occur in the dynamic range of the contrast response function (Reynolds, Pasternak, & Desimone, 2000). We found that overt attention also altered the contrast response function in MT, but in our data set, the effect size was fairly constant across the range of contrasts; this may be more consistent with exogenous attentional cueing, which has been reported to produce a mix of contrast and response gain, measured psychophysically (Ling & Carrasco, 2006). Covert attention was originally reported to reduce noise correlations between neurons in V4 (Cohen & Maunsell, 2009); baseline noise correlations in this study were positive, consistent with our observations of decreases in correlations for pairs of MT neurons whose baseline visual correlation was positive. Subsequent work has revealed that changes in noise correlations during covert attention can depend on task demands (Ruff & Cohen, 2014). Overall, we found that the neural changes observed when saccade is directed toward the neurons' RF resemble those previously reported in the covert attention literature, emphasizing the similarities between the overt and covert attention, and shared mechanisms of the saccade and attention systems.

In order to compare the influence of covert and overt attention on neural representations, we compare our results on the relative contribution of rate and variability changes to population information with those obtained during covert attention (Cohen & Maunsell, 2009). The condition most analogous to Cohen and Maunsell's analysis of covert attention in V4 is our comparison of motion direction discriminability (however, we should note that their study used ensembles of tens of neurons, rather than pairs, for d' calculations). Like that study, we found that changes in noise correlations between neurons contribute to enhancing the stimulus representation; however, we also found substantial contributions from the rate and reliability components. This discrepancy might reflect differences based on neural ensemble size, brain area (V4 vs. MT), or type of attention (overt vs. covert).

Our finding that perisaccadic changes in rate and noise correlations contribute differently to the representation of motor and visual information is interesting in light of several other recent findings. We have previously shown that inactivating FEF increases perisaccadic FRs in V4, but decreases the orientation selectivity of that activity (Noudoost, Clark, & Moore, 2014). We have also recently reported that motor activity is rare in FEF neurons projecting to extrastriate visual cortex (Merrikhi et al., 2017). Taken together, these findings suggest a model in which FEF input to extrastriate areas drives increased visual selectivity in these areas, both during overt or covert attention, primarily by changing the noise correlations between neurons. The rate changes, in contrast, are driven at least in part by another area with motor activity (e.g., superior colliculus), reflect primarily motor preparation, and make less contribution to the stimulus representation. This dissociation of (primarily) rate-based motor modulation and variability-based selectivity modulation supports a model in which input from FEF enhances extrastriate visual representations during both overt and covert attention, but another source drives motor modulation.

Reprint requests should be sent to Yaser Merrikhi, Department of Physiology, McGill University, Montréal, QC H3G 1Y6, Canada, or via e-mail: yaser.merrikhiahangarkolaee@mcgill.ca.

Author Contributions

Y. M., M. S. and B. N. designed the experiment; Y. M. and B. N. performed the experiments; Y. M., M. S., H. K., R. E. and B. N. analyzed the data; Y. M., K. C., R. E. and B. N. wrote the manuscript.

Funding Information

This work was supported by the National Institutes of Health, grant numbers: R01EY026924, R01MH121435, R01NS113073 to B. N. and an Unrestricted Grant from Research to Prevent Blindness, Inc. to Moran Eye Center, University of Utah.

Diversity in Citation Practices

A retrospective analysis of the citations in every article published in this journal from 2010 to 2020 has revealed a persistent pattern of gender imbalance: Although the proportions of authorship teams (categorized by estimated gender identification of first author/last author) publishing in the *Journal of Cognitive Neuroscience (JoCN)* during this period were M(an)/M = .408, W(oman)/M = .335, M/W = .108, and W/W = .149, the comparable proportions

for the articles that these authorship teams cited were M/M = .579, W/M = .243, M/W = .102, and W/W = .076 (Fulvio et al., *JoCN*, 33:1, pp. 3–7). Consequently, *JoCN* encourages all authors to consider gender balance explicitly when selecting which articles to cite and gives them the opportunity to report their article's gender citation balance.

REFERENCES

Asaad, W. F., Santhanam, N., McClellan, S., & Freedman, D. J. (2013). High-performance execution of psychophysical tasks with complex visual stimuli in MATLAB. *Journal of Neurophysiology*, *109*, 249–260. https://doi.org/10.1152/jn.00527.2012, PubMed: 23034363

Awh, E., Armstrong, K. M., & Moore, T. (2006). Visual and oculomotor selection: Links, causes and implications for spatial attention. *Trends in Cognitive Sciences*, *10*, 124–130. https://doi.org/10.1016/j.tics.2006.01.001, PubMed: 16469523

Born, S., Ansorge, U., & Kerzel, D. (2013). Predictability of spatial and non-spatial target properties improves perception in the pre-saccadic interval. *Vision Research*, *91*, 93–101. https://doi.org/10.1016/J.VISRES.2013.08.003, PubMed: 23954813

Bremmer, F., Kubischik, M., Hoffmann, K.-P., & Krekelberg, B. (2009). Neural dynamics of saccadic suppression. *Journal of Neuroscience*, *29*, 12374–12383. https://doi.org/10.1523/JNEUROSCI.2908-09.2009, PubMed: 19812313

Chelazzi, L., Miller, E. K., Duncan, J., & Desimone, R. (1993). A neural basis for visual search in inferior temporal cortex. *Nature*, *363*, 345–347. https://ramsesii.upf.es/seminar/ChelazziMDD1993.pdf. https://doi.org/10.1038/363345a0, PubMed: 8497317

Chelazzi, L., Miller, E. K., Duncan, J., & Desimone, R. (2001). Responses of neurons in macaque area V4 during memory-guided visual search. *Cerebral Cortex*, *11*, 761–772. https://doi.org/10.1093/cercor/11.8.761, PubMed: 11459766

Churchland, M. M., Yu, B. M., Cunningham, J. P., Sugrue, L. P., Cohen, M. R., Corrado, G. S., et al. (2010). Stimulus onset quenches neural variability: A widespread cortical phenomenon. *Nature Neuroscience*, *13*, 369–378. https://doi.org/10.1038/nn.2501, PubMed: 20173745

Cohen, M. R., & Maunsell, J. H. (2009). Attention improves performance primarily by reducing interneuronal correlations. *Nature Neuroscience*, *12*, 1594–1600. https://doi.org/10.1038/nn.2439, PubMed: 19915566

Deubel, H., & Schneider, W. X. (1996). Saccade target selection and object recognition: Evidence for a common attentional mechanism. *Vision Research*, *36*, 1827–1837. https://doi.org/10.1016/0042-6989(95)00294-4, PubMed: 8759451

Ecker, A. S., Berens, P., Tolias, A. S., & Bethge, M. (2011). The effect of noise correlations in populations of diversely tuned neurons. *Journal of Neuroscience*, *31*, 14272–14283. https://doi.org/10.1523/JNEUROSCI.2539-11.2011, PubMed: 21976512

Fischer, B., & Boch, R. (1981). Selection of visual targets activates prelunate cortical cells in trained rhesus monkey. *Experimental Brain Research*, *41*, 431–433. https://doi.org/10.1007/BF00238903, PubMed: 7215505

Hafed, Z. M., & Chen, C. Y. (2016). Sharper, stronger, faster upper visual field representation in primate superior colliculus. *Current Biology*, *26*, 1647–1658. https://doi.org/10.1016/j.cub.2016.04.059, PubMed: 27291052

Hanning, N. M., Jonikaitis, D., Deubel, H., & Szinte, M. (2016). Oculomotor selection underlies feature retention in visual working memory. *Journal of Neurophysiology*, *115*, 1071–1076. https://doi.org/10.1152/jn.00927.2015, PubMed: 26581875

Hoffman, J. E., & Subramaniam, B. (1995). The role of visual attention in saccadic eye movements. *Perception & Psychophysics*, *57*, 787–795. https://doi.org/10.3758/BF03206794, PubMed: 7651803

Hu, Y., Zylberberg, J., & Shea-Brown, E. (2014). The sign rule and beyond: Boundary effects, flexibility, and noise correlations in neural population codes. *PLoS Computational Biology*, *10*, e1003469. https://doi.org/10.1371/journal.pcbi.1003469, PubMed: 24586128

Kohn, A., Coen-Cagli, R., Kanitscheider, I., & Pouget, A. (2016). Correlations and neuronal population information. *Annual Review of Neuroscience*, *39*, 237–256. https://doi.org/10.1146/annurev-neuro-070815-013851, PubMed: 27145916

Ling, S., & Carrasco, M. (2006). Sustained and transient covert attention enhance the signal via different contrast response functions. *Vision Research*, *46*, 1210–1220. https://doi.org/10.1016/j.visres.2005.05.008, PubMed: 16005931

McAdams, C. J., & Maunsell, J. H. (1999). Effects of attention on orientation-tuning functions of single neurons in macaque cortical area V4. *Journal of Neuroscience*, *19*, 431–441. https://doi.org/10.1523/JNEUROSCI.19-01-00431.1999, PubMed: 9870971

Merrikhi, Y., Clark, K., Albarran, E., Parsa, M., Zirnsak, M., Moore, T., et al. (2017). Spatial working memory alters the efficacy of input to visual cortex. *Nature Communications*, *8*, 15041. https://doi.org/10.1038/ncomms15041, PubMed: 28447609

Merrikhi, Y., Clark, K. L., & Noudoost, B. (2018). Concurrent influence of top–down and bottom-up inputs on correlated activity of Macaque extrastriate neurons. *Nature Communications*, *9*, 5393. https://doi.org/10.1038/s41467-018-07816-4, PubMed: 30568166

Mitchell, J. F., Sundberg, K. a., & Reynolds, J. H. (2007). Differential attention-dependent response modulation across cell classes in macaque visual area V4. *Neuron*, *55*, 131–141. https://doi.org/10.1016/j.neuron.2007.06.018, PubMed: 17610822

Montemurro, M. A., & Panzeri, S. (2006). Optimal tuning widths in population coding of periodic variables. *Neural Computation*, *18*, 1555–1576. https://doi.org/10.1162/neco.2006.18.7.1555, PubMed: 16764514

Moore, T. (1999). Shape representations and visual guidance of saccadic eye movements. *Science*, *285*, 1914–1917. https://doi.org/10.1126/science.285.5435.1914, PubMed: 10489371

Moore, T., & Chang, M. H. (2009). Presaccadic discrimination of receptive field stimuli by area V4 neurons. *Vision Research*, *49*, 1227–1232. https://doi.org/10.1016/j.visres.2008.03.018, PubMed: 18501949

Moore, T., Tolias, A. S., & Schiller, P. H. (1998). Visual representations during saccadic eye movements. *Proceedings of the National Academy of Sciences, U.S.A.*, *95*, 8981–8984. https://doi.org/10.1073/pnas.95.15.8981, PubMed: 9671790

Moran, J., & Desimone, R. (1985). Selective attention gates visual processing in the extrastriate cortex. *Science*, *229*, 782–784. https://www.sciencemag.org/content/229/4715/782.short. https://doi.org/10.1126/science.4023713, PubMed: 4023713

Neupane, S., Guitton, D., & Pack, C. C. (2016a). Dissociation of forward and convergent remapping in primate visual cortex. *Current Biology*, *26*, R491–R492. https://doi.org/10.1016/j.cub.2016.04.050, PubMed: 27326707

Neupane, S., Guitton, D., & Pack, C. C. (2016b). Two distinct types of remapping in primate cortical area V4. *Nature*

Communications, *7*, 10402. https://doi.org/10.1038/ncomms10402, PubMed: 26832423

Noudoost, B., Clark, K. L., & Moore, T. (2014). A distinct contribution of the frontal eye field to the visual representation of saccadic targets. *Journal of Neuroscience*, *34*, 3687–3698. https://doi.org/10.1523/JNEUROSCI.3824-13.2014, PubMed: 24599467

Peterson, M. S., Kramer, A. F., & Irwin, D. E. (2004). Covert shifts of attention precede involuntary eye movements. *Perception & Psychophysics*, *66*, 398–405. https://doi.org/10.3758/BF03194888, PubMed: 15283065

Ponce-Alvarez, A., Thiele, A., Albright, T. D., Stoner, G. R., & Deco, G. (2013). Stimulus-dependent variability and noise correlations in cortical MT neurons. *Proceedings of the National Academy of Sciences, U.S.A.*, *110*, 13162–13167. https://doi.org/10.1073/pnas.1300098110, PubMed: 23878209

Reynolds, J. H., Pasternak, T., & Desimone, R. (2000). Attention increases sensitivity of V4 neurons. *Neuron*, *26*, 703–714. https://doi.org/10.1016/S0896-6273(00)81206-4, PubMed: 10896165

Rolfs, M., & Carrasco, M. (2012). Rapid simultaneous enhancement of visual sensitivity and perceived contrast during saccade preparation. *Journal of Neuroscience*, *32*, 13744–13752. https://doi.org/10.1523/JNEUROSCI.2676-12.2012, PubMed: 23035086

Ruff, D. A., & Cohen, M. R. (2014). Attention can either increase or decrease spike count correlations in visual cortex. *Nature Neuroscience*, *17*, 1591–1597. https://doi.org/10.1038/nn.3835, PubMed: 25306550

Seriès, P., Latham, P. E., & Pouget, A. (2004). Tuning curve sharpening for orientation selectivity: Coding efficiency and the impact of correlations. *Nature Neuroscience*, *7*, 1129–1135. https://doi.org/10.1038/nn1321, PubMed: 15452579

Shadlen, M. N., Britten, K. H., Newsome, W. T., & Movshon, J. A. (1996). A computational analysis of the relationship between neuronal and behavioral responses to visual motion. *Journal of Neuroscience*, *16*, 1486–1510. https://doi.org/10.1523/JNEUROSCI.16-04-01486.1996, PubMed: 8778300

Sheinberg, D. L., & Logothetis, N. K. (2001). Noticing familiar objects in real world scenes: The role of temporal cortical neurons in natural vision. *Journal of Neuroscience*, *21*, 1340–1350. https://doi.org/10.1523/JNEUROSCI.21-04-01340.2001, PubMed: 11160405

Spitzer, H., Desimone, R., & Moran, J. (1988). Increased attention enhances both behavioral and neuronal performance. *Science*, *240*, 338–340. https://doi.org/10.1126/science.3353728, PubMed: 3353728

Steinmetz, N. A., & Moore, T. (2010). Changes in the response rate and response variability of area V4 neurons during the preparation of saccadic eye movements. *Journal of Neurophysiology*, *103*, 1171–1178. https://doi.org/10.1152/jn.00689.2009, PubMed: 20018834

Steinmetz, N. A., & Moore, T. (2014). Eye movement preparation modulates neuronal responses in area V4 when dissociated from attentional demands. *Neuron*, *83*, 496–506. https://doi.org/10.1016/j.neuron.2014.06.014, PubMed: 25033188

Stewart, E. E. M., Verghese, P., & Ma-Wyatt, A. (2019). The spatial and temporal properties of attentional selectivity for saccades and reaches. *Journal of Vision*, *19*, 12. https://doi.org/10.1167/19.9.12, PubMed: 31434108

Thiele, A., Henning, P., Kubischik, M., & Hoffmann, K.-P. (2002). Neural mechanisms of saccadic suppression. *Science*, *295*, 2460–2462. https://doi.org/10.1126/science.1068788, PubMed: 11923539

Tolias, A. S., Moore, T., Smirnakis, S. M., Tehovnik, E. J., Siapas, A. G., & Schiller, P. H. (2001). Eye movements modulate visual receptive fields of V4 neurons. *Neuron*, *29*, 757–767. https://doi.org/10.1016/S0896-6273(01)00250-1, PubMed: 11301034

Treue, S., & Maunsell, J. H. (1996). Attentional modulation of visual motion processing in cortical areas MT and MST. *Nature*, *382*, 539–541. https://doi.org/10.1038/382539a0, PubMed: 8700227

Zirnsak, M., Steinmetz, N. A., Noudoost, B., Xu, K. Z., & Moore, T. (2014). Visual space is compressed in prefrontal cortex before eye movements. *Nature*, *507*, 504–507. https://doi.org/10.1038/nature13149, PubMed: 24670771